

# RSC Advances



This is an *Accepted Manuscript*, which has been through the Royal Society of Chemistry peer review process and has been accepted for publication.

*Accepted Manuscripts* are published online shortly after acceptance, before technical editing, formatting and proof reading. Using this free service, authors can make their results available to the community, in citable form, before we publish the edited article. This *Accepted Manuscript* will be replaced by the edited, formatted and paginated article as soon as this is available.

You can find more information about *Accepted Manuscripts* in the [Information for Authors](#).

Please note that technical editing may introduce minor changes to the text and/or graphics, which may alter content. The journal's standard [Terms & Conditions](#) and the [Ethical guidelines](#) still apply. In no event shall the Royal Society of Chemistry be held responsible for any errors or omissions in this *Accepted Manuscript* or any consequences arising from the use of any information it contains.

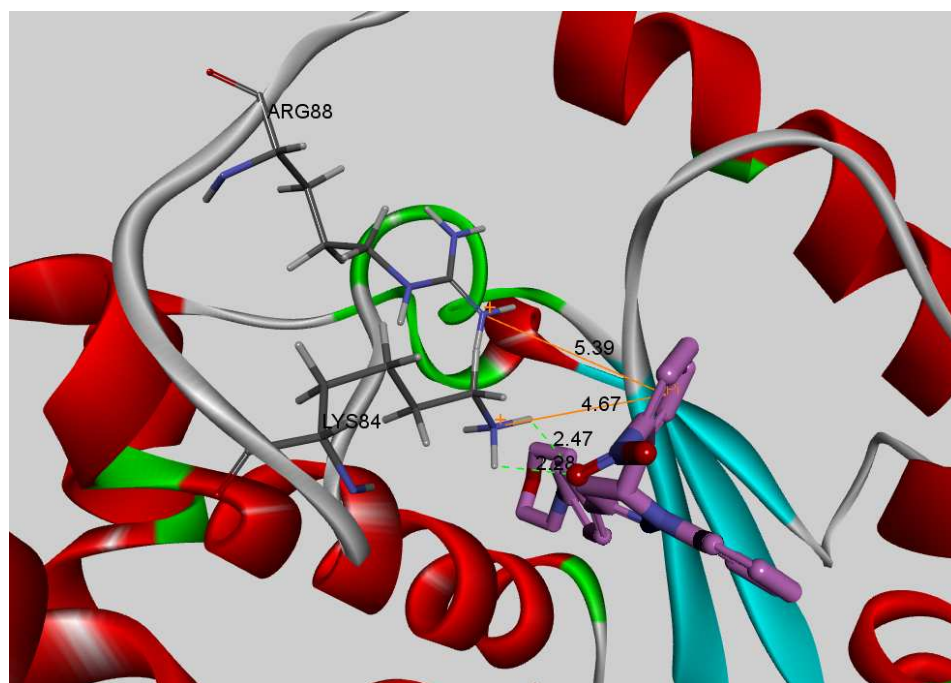
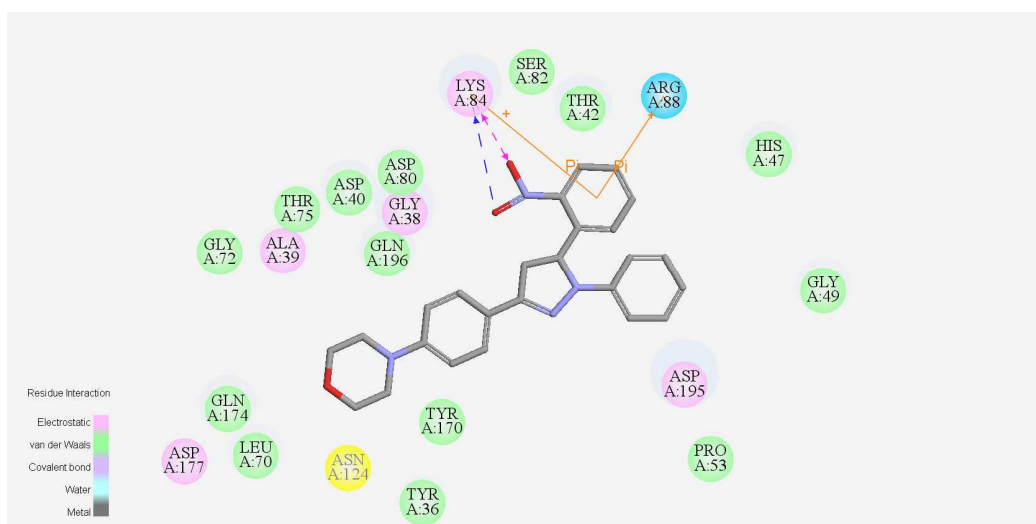
# Dihydropyrazoles Containing Morpholine: Design, Synthesis and Bioassay as Potent Antimicrobial Agents

Peng-Fei Wang, Han-Yue Qiu, Xiao-Qiang Yan, Long-Wang Chen, Xiao-Yuan

Lu, Zhong-Chang Wang\*, Hai-Liang Zhu\*

*State Key Laboratory of Pharmaceutical Biotechnology, Nanjing University, Nanjing*

*210093, People's Republic of China*



A series of dihydropyrazole derivatives containing morpholine was designed and synthesized as antimicrobial agents. In both docking simulation and bioassay test, these compounds showed potent *S. aureus* TyrRS enzyme inhibition activity, holding the promise of being developed as potential drugs.

# **Dihydropyrazoles Containing Morpholine: Design, Synthesis and Bioassay as Potent Antimicrobial Agents**

**Peng-Fei Wang<sup>a</sup>, Han-Yue Qiu<sup>a</sup>, Jun-Ting Ma<sup>a</sup>, Xiao-Qiang Yan<sup>a</sup>,**

**Hai-Bin Gong<sup>a,b,\*</sup>, Zhong-Chang Wang<sup>a,\*</sup>, Hai-Liang Zhu<sup>a,\*</sup>**

*<sup>a</sup>State Key Laboratory of Pharmaceutical Biotechnology, Nanjing University, Nanjing  
210093, People's Republic of China*

*<sup>b</sup>Xuzhou Central Hospital, Xuzhou 221009, People's Republic of China*

RSC Advances Accepted Manuscript

\*Corresponding author. Tel. & fax: +86-25-83592672; e-mail: [zhuhl@nju.edu.cn](mailto:zhuhl@nju.edu.cn)

**Abstract**

A series of dihydropyrazole derivatives containing morpholine was designed and synthesized as antimicrobial agents. All of the synthesized compounds were determined by  $^1\text{H-NMR}$  and MS. Afterwards they were evaluated for *in vitro* antibacterial activity against four bacteria strains. Along with the *S. aureus* TyrRS inhibition and cytotoxicity examination, some compounds proved to be low-toxic and potent, especially against Gram-positive bacteria strains. Compound **4s** exhibited the potential to be new antibacterial drug with strong broad-spectrum antimicrobial activity and enzyme inhibitory activity. Docking simulation was performed to position compound **4s** into the *S. aureus* TyrRS structure active site to investigate the probable binding mode. A 3D-QSAR model was also established to explain how structural alterations affect the activity and guide the further study.

**Keywords:**

Dihydropyrazole

Antibacterial

TyrRS

Docking

3D-QSAR

## 1 Introduction

It has long been researched and exploited for clinical use since the first emerge of antibiotic in 1930s; to date numerous improved analogues are available.<sup>1</sup> However, after years of misuse, overuse and misdiagnosis, traditional clinical antibiotics tend to be feeble in face of remarkably increasing resistance of microbes.<sup>2</sup> By mutant in the binding site or directly bypassing the target functionally or being impermeable, bacteria acquired the resistance to traditional drugs cunningly.<sup>3</sup> Along with the resistance was the advent of higher rates of morbidity and mortality, putting forward severe challenge to medicine research and development.<sup>4,5</sup> Therapeutic targets should be further studied and new antimicrobial drugs elaborated to ease the intensified contradiction between supply and demand.

As the relevant theories developed and practice research got deeper, however, it tended to be that the traditional antibacterial targets still maintain their dominant position in drug design area, for the molecular screening of new genomic targets turned out to be lackluster.<sup>6</sup> Among all the validated targets, aminoacyl tRNA synthetases (aaRSs) stand for one class of the most potential. The aaRSs are essential enzymes catalyzing the charging of tRNA, which was a vital process in the translation of mRNA into protein.<sup>7</sup> The catalysis was performed with high fidelity, to assure the correct amino acid loaded to the tRNA and concomitantly making these enzymes highly conserved in catalytic domains. They are found in all kinds of lives for their indispensability and many vary in sequence between prokaryotes and eukaryotes.<sup>3</sup> Taken all these factors (essential, conserved and different between prokaryotes and eukaryotes) into consideration, it's clear that the aaRSs family provides ideal and potential targets for antibacterial drugs. However, these enzymes remain underexploited for only Bactroban (also known as mupirocin) targeting isoleucin-tRNA synthetase (IleRS) has been approved as antibiotics in clinical use. Research on the utilization of aaRSs as antibacterial targets has broad space and paves the way for the designing of antimicrobial drugs. As part of the huge aaRSs family, tyrosyl-tRNA synthetase (TyrRS) holds importance to the protein synthesis and has already received close attention. It functions differently between human being and

microbes and this means that as antibacterial agents, drugs targeting TyrRS would gain low toxicity to normal cells.<sup>8</sup> Now the TyrRS family has been validated as a promising target against the bacteria with rising resistance, and corresponding antagonists are being developed to meet the substantial clinical need.

As a kind of nitrogen-containing heterocycle, morpholine received significant attention for their broad spectrum purposes. It has been investigated that many morpholines possess the bioactivities of anticancer,<sup>9</sup> antimicrobial,<sup>10</sup> acesodyne,<sup>11</sup> anti-inflammatory,<sup>12</sup> antiemetic<sup>13</sup> and so on. The block of morpholine is essential in many clinical medicines like Gefitinib (Iressa), Linezolid, Pinaverium Bromide and Buparlisib (**Figure 1**). Also, pyrazolines are of various activities and have versatile use in medicinal chemistry. Among all the multitudinous pyrazoline derivatives, substituted dihydropyrazoles performed particularly well in manifold applications, including antitumor,<sup>14</sup> anti-depressant,<sup>15</sup> immunosuppression,<sup>16</sup> antituberculous,<sup>17</sup> anti-inflammatory,<sup>18</sup> antidiabetic,<sup>19</sup> antibacteria,<sup>20</sup> antimalarial,<sup>21</sup> antiamebic.<sup>22</sup> The significance dihydropyrazoles hold to pharmacy led to increasing interests and keep them valuable in drug design. In our previous work, several series of pyrazole compounds have been synthesized and bioassays have proved some possess potent bioactivity and low toxicity.<sup>23</sup> TryRS has also been exploited as antibacterial target to examine the bioactivity of synthesis and based on these former research studies, the nitrogen atom-containing heterocyclic structurally resembling morpholine was found vital.<sup>8,24</sup> Thus it was of interest to implement the symbiotic approach to design novel candidates linking morpholine to dihydropyrazoles and investigate their bioactivity.

In this research, we have designed and synthesized a class of dihydropyrazoles bearing morpholine ring as antibacterial drug. Succeeding bioactivity assay suggested these compounds possess potent antibacterial activity, especially against Gram-positive bacteria strains. The *S. aureus* TyrRS inhibition and cytotoxicity examination suggest these compounds are potent antagonists and low-toxic. Furthermore, docking simulations were performed using the X-ray crystallographic structure of the *S. aureus* TryRS (PDB code: 1JII) to explore the binding modes of these compounds at the active site. A 3D-QSAR model was achieved in order to

explain how structural alterations impact the activity, paving the way for further study.

## 2 Results and Discussion

### 2.1 Chemistry

The synthetic process of the 20 compounds followed the route depicted in **Scheme 1**. To a stirred solution of morpholine in DMSO, *p*-fluorobenzaldehyde was added and the reaction was heated for 4 h, poured into ice water to give compound **2**. The chalcones **3a-3t** were gained by the condensation of compound **2** and various acetophenone, in ice bath and catalyzed by KOH. Under stirring, the chalcones were added into acetic acid along with phenylhydrazine. The reaction was then heated to reflux and furnished compounds **4a-4t**. All of the target compounds **4a-4t** are reported for the first time, and give satisfactory analytical and spectroscopic data. <sup>1</sup>HNMR and EI-MS spectra were consistent with the assigned structures.

### 2.2 Biological activity

#### 2.2.1 Antibacterial activity

Two Gram-negative bacterial strains: *E. coli* and *P. aeruginosa* and two Gram-positive bacterial strains: *B. subtilis* and *S. aureus* were exploited in the antimicrobial assay. The test followed the MIC method and took Penicillin and Kanamycin under identical conditions as control. The results were listed in **Table 1**, and as shown, the MIC (minimum inhibitory concentration) value indicated that some of the new synthetic possess potent activity compared to the control. On the whole, these compounds are stronger antagonists of Gram-positive bacterial strains than Gram-negative. Against *S. aureus*, compounds **4b**, **4c**, **4e**, **4p**, **4q** and **4t** (each with MIC of 3.13  $\mu\text{g/mL}$ ) are comparable to Penicillin (MIC of 3.13  $\mu\text{g/mL}$ ). Compounds **4e**, **4f**, and **4t** (MIC of 1.56 to 3.13  $\mu\text{g/mL}$ ) are comparable to Penicillin (MIC of 3.13  $\mu\text{g/mL}$ ) and Kanamycin (MIC of 1.56  $\mu\text{g/mL}$ ). Notably, compound **4s** showed broad-spectrum antibacterial activity against all the four bacteria strains, with MIC of 0.78 to 3.13  $\mu\text{g/mL}$ . The result suggested this compound was more potent than Penicillin and Kanamycin overall. Though other compounds are less potent, many are close to the

control. To enhance the antiseptic activity against *S. aureus*, electron-drawing groups tended to be preferable than electron-donating groups. This conclusion is especially suitable when it comes to the *o*-position substitutes, for the order of electron-drawing potential is:  $-\text{NO}_2 > -\text{F} > -\text{Cl} > -\text{H}$  and the order of antibacterial potential is **4s** > **4b** > **4g** > **4a**. Also, **4s**, **4b** and **4g** are more potent than **4m** and **4p** which have electron-donating group on *o*-position.

### 2.2.2 *S. aureus* TyrRS enzyme inhibition

The *S. aureus* TyrRS enzyme inhibitory activity of these compounds was investigated and the result was summarized in **Table 2**. As shown, to some extent the potential of antibacterial is consistent to the enzyme inhibition of *S. aureus* TyrRS, with a few exceptions. In detail, compounds possessing potent activity against *S. aureus* are generally endowed with significant potential against the enzyme *S. aureus* TyrRS; compounds **4b**, **4c**, **4e**, **4t** and **4s** inflicting more destruction to bacteria (with MIC of 0.78 to 3.13  $\mu\text{g}/\text{mL}$ ) possess relatively more potent inhibition to *S. aureus* TyrRS (with  $\text{IC}_{50}$  of 1.63 to 24.1  $\mu\text{M}$ ). On the other hand, compounds **4a**, **4n**, **4g**, **4i**, **4j** and **4l** bearing lower antimicrobial properties (with MIC of 12.5 to 25  $\mu\text{g}/\text{mL}$ ) gain poor enzyme inhibition activity (with  $\text{IC}_{50}$  of 18.13 to 48.79  $\mu\text{M}$ ). From the data listed, a conclusion similar to the one above could be achieved for there's consistency between antibacterial activity and *S. aureus* TyrRS enzyme inhibition with little discrepancy: electron-drawing groups are preferable than electron-donating groups. Besides, taken electron-drawing groups into consideration, it can be concluded that substitutes on *o*-position and *m*-position make for the potential, as compounds **4b** and **4c** are more potent than **4d** (with  $\text{IC}_{50}$  of 11.92, 4.53, 15.27  $\mu\text{M}$ , respectively). It's also supported by compounds **4i**, **4h**, and **4g** (with  $\text{IC}_{50}$  of 32.22, 24.1, 30.73  $\mu\text{M}$ , respectively).

### 2.2.3 Cytotoxicity

To examine the safety of these compounds, all of the new compounds were evaluated for their toxicity against the human kidney epithelial cell 293T (median cytotoxic concentration ( $\text{CC}_{50}$ ) data) using the MTT assay.<sup>25</sup> As shown in **Table 2**,  $\text{IC}_{50}$  value

was employed to demonstrate the harm to 293T cells caused by these compounds and the result turned out to be favorable.

### 2.3 Docking

Docking is an effective and reliable approach to simulate the probable binding mode of ligands and proteins. In this study, we have performed the docking study by fitting the most potent compound **4s** into the active center of the *S. aureus* TyrRS (PDB code: 1JJJ) using Discovery Studio 3.5. The results obtained are presented in Figure 2 and 3. As showed, two amino acids, **LYS84** and **ARG88**, are of significance in the binding of ligand with enzyme; especially the **LYS84** forms a cation- $\pi$  interaction, a electrostatic interaction and two hydrogen bonds with **4s** (angle O · H-N = 104.1°, distance = 2.28 Å; angle O · H-N = 92.5°, distance = 2.48 Å; however, in the 2D graph, these two hydrogen bonds are overlapped, which could be distinguished in the 3D graph), while a cation- $\pi$  interaction was formed between **ARG88** and **4s**. The molecular docking results, along with the biological assay data, suggest that compound **4s** is a potential inhibitor of *S. aureus* TyrRS.

### 2.4 3D-QSAR model

In consideration of making for follow-up research, a 3D-QASR model was built to study the systematic structure-activity relationship of these compounds. As intended, analysis and improvement suggestions should be gained by the 3D-QASR model, which plays significant role in guidance of seeking for more powerful antagonists against *S. aureus* TyrRS. The process was carried out by built-in QSAR software of DS 3.5 (Discovery Studio 3.5, Accelrys, Co. Ltd), with all molecules converted to the active conformation and corresponding pIC<sub>50</sub> ( $\mu$ M) values. Concomitantly, these compounds were randomly partition into two groups: training set and test set. While the training set contains 80% of these compounds, the test set comprise the rest four agents, as summarized in **Table 3**.

By default, each molecule was arranged to possess alignment conformation with the lowest CDOCKER\_INTERACTION\_ENERGY among all of the docked poses while

CHARMm force field and PLS regression were exerted in building of 3D-QSAR model. As showed in **Figure 4**, a scatter plot with conventional  $R^2$  of 0.816 was gained, indicating a high degree of compatibility exists between the predicted  $pIC_{50}$  and actual  $pIC_{50}$ ; hence this model possesses reliable predicting capability. Also, the information of critical regions (steric or electrostatic) affecting the binding affinity was gained: all of the compounds were aligned with the iso-surfaces of the 3D-QSAR model coefficients on electrostatic potential grids (**Figure 5 (a)**) and Van der Waals grids (**Figure 5 (b)**). The electrostatic map presents the information of favorable (in blue) or unfavorable (in red) electrostatic field regions in a contour plot, while the energy grids corresponding to the favorable (in green) or unfavorable (in yellow) steric effects are also marked out. It's characterized as active for compounds bearing strong Van der Waals attraction in the green areas and polar groups in the blue electrostatic potential areas. A good compliance is observed between the model and actual situation for compounds under study. On the base of this part of study, optimized compounds possessing more potential against enzyme *S. aureus* TyrRS could be designed, with the activity easily and credibly predicated.

### 3 Conclusion

In this study, a suite of new *S. aureus* TyrRS inhibitors has been designed and synthesized; their potential has been evaluated in the following bioassays, which suggest these compounds possess moderate to potent antibacterial activity and *S. aureus* TyrRS inhibitory activity. The cytotoxicity test employing human kidney epithelial cell 293T also indicates high safety. Among all these compounds, compound **4s** showed the most potent inhibition activity against four bacteria strains (with MIC of 1.56, 0.78, 3.13, 1.56  $\mu\text{g}/\text{mL}$ ) and *S. aureus* TyrRS enzyme (with  $IC_{50}$  of 1.63  $\mu\text{M}$ ). The probable binding mode proposed by the docking simulation may be a good explanation of the impressive performance of **4s**, in which **4s** binds well with *S. aureus* TyrRS via two hydrogen bonds and two cation- $\pi$  interactions. In addition, a reliable 3D-QSAR model was gained to analyze the structure-activity relationship, and make for the further study seeking for more potent agents against *S. aureus*

TyrRS.

## 4 Experiments

### 4.1 Materials and measurements

All chemicals and reagents used in current study were analytical grade. All the  $^1\text{H}$ NMR spectra were recorded on a Bruker DPX 400 model Spectrometer in  $\text{DMSO-}d_6$  and chemical shifts ( $\delta$ ) were reported as parts per million (ppm). EI-MS spectra were recorded a Mariner System 5304 Mass spectrometer. Melting points were determined on a XT4 MP apparatus (Taike Corp, Beijing, China). Thin layer chromatography (TLC) was performed on silica gel plates (Silica Gel 60 GF254) and visualized in UV light (254 nm). Column chromatography was performed using silica gel (200-300 mesh) eluting with ethyl acetate and petroleum ether.

### 4.2 General procedure for preparation of compound 2

Under stirring, morphine (50 mmol) was added to DMSO (20 mL); afterwards equivalent *p*-fluorobenzaldehyde was added into the solution. The reaction was heated to reflux for 4 h, and then poured into mass ice water to give the yellow precipitate. The crude product was then washed by cold ethanol and water for three times to give compound 2.

### 4.3 General procedure for preparation of compounds 3a-3t

The compound 2 was then added and dissolved in 20 mL ethanol, along with equivalent substituted acetophenone. The solution was then removed to ice bath and stirred. After 5 min, 3 equivalent KOH was added slowly into the reaction, which was poured into saturated salt water to give crude product in 2 h. The product was then washed by cold ethanol and water for three times to give compounds 3a-3t.

### 4.4 General procedure for preparation of compounds 4a-4t

To a stirred solution of compound 3a-3t in 20 mL acetic acid, 1.2 equivalent phenylhydrazine was added dropwise; the reaction was then heated to reflux for 6 h

and ended by poured into ice water, furnishing the target compounds **4a-4t** purified by column chromatography subsequently.

#### 4.4.1 4-(4-(1,5-Diphenyl-4,5-dihydro-1H-pyrazol-3-yl)phenyl)morpholine (**4a**)

Yellow crystal, yield 67.1%, m.p. 184-186 °C. <sup>1</sup>H NMR (400 MHz, DMSO-*d*<sub>6</sub>) δ 7.79 – 7.70 (m, 2H, ArH), 7.47 – 7.34 (m, 3H, ArH), 7.15 (dt, *J* = 8.6, 3.5 Hz, 4H, ArH), 7.03 (d, *J* = 7.8 Hz, 2H, ArH), 6.90 (d, *J* = 8.7 Hz, 2H, ArH), 6.71 (t, *J* = 7.2 Hz, 1H, ArH), 5.39 (dd, *J* = 12.1, 6.3 Hz, 1H, CH), 3.87 (dd, *J* = 17.4, 12.2 Hz, 1H, CH<sub>2</sub>), 3.72 – 3.68 (m, 4H, CH<sub>2</sub>), 3.10 (d, *J* = 6.3 Hz, 1H, CH<sub>2</sub>), 3.08 – 3.03 (m, 4H, CH<sub>2</sub>). MS (EI): 383.1 (M<sup>+</sup>).

#### 4.4.2

#### 4-(4-(5-(2-Fluoro)-1-phenyl-4,5-dihydro-1H-pyrazol-3-yl)phenyl)morpholine (**4b**)

Yellow crystal, yield 55.7%, m.p. 141-143 °C. <sup>1</sup>H NMR (400 MHz, DMSO-*d*<sub>6</sub>) δ 7.96 – 7.87 (m, 1H, ArH), 7.41 (td, *J* = 7.2, 3.5 Hz, 1H, ArH), 7.31 – 7.23 (m, 2H, ArH), 7.16 (t, *J* = 8.0 Hz, 4H, ArH), 7.03 (d, *J* = 7.8 Hz, 2H, ArH), 6.90 (d, *J* = 8.7 Hz, 2H, ArH), 6.73 (t, *J* = 7.3 Hz, 1H, ArH), 5.40 (dd, *J* = 12.2, 6.3 Hz, 1H, CH), 3.94 (dd, *J* = 16.4, 12.4 Hz, 1H, CH<sub>2</sub>), 3.73 – 3.64 (m, 4H, CH<sub>2</sub>), 3.13 (dd, *J* = 6.3, 2.1 Hz, 1H, CH<sub>2</sub>), 3.11 – 3.04 (m, 4H, CH<sub>2</sub>). MS (EI): 401.2 (M<sup>+</sup>).

#### 4.4.3

#### 4-(4-(5-(3-Fluorophenyl)-1-phenyl-4,5-dihydro-1H-pyrazol-3-yl)phenyl)morpholine (**4c**)

Yellow crystal, yield 78.3%, m.p. 140-141 °C. <sup>1</sup>H NMR (400 MHz, DMSO-*d*<sub>6</sub>) δ 7.64 (d, *J* = 8.1 Hz, 2H, ArH), 7.24 (d, *J* = 8.0 Hz, 2H, ArH), 7.17 – 7.12 (m, 4H, ArH), 7.03 – 6.99 (m, 2H, ArH), 6.89 (d, *J* = 8.8 Hz, 2H, ArH), 6.70 (t, *J* = 7.2 Hz, 1H, ArH), 5.35 (dd, *J* = 12.0, 6.3 Hz, 1H, CH), 3.83 (dd, *J* = 17.4, 12.1 Hz, 1H, CH<sub>2</sub>), 3.71 (dd, *J* = 11.3, 7.0 Hz, 4H, CH<sub>2</sub>), 3.09 – 2.98 (m, 5H, CH<sub>2</sub>). MS (EI): 401.2 (M<sup>+</sup>).

#### 4.4.4

#### 4-(4-(5-(4-Fluorophenyl)-1-phenyl-4,5-dihydro-1H-pyrazol-3-yl)phenyl)morpholine (**4d**)



= 8.7 Hz, 2H, ArH), 6.73 (t,  $J$  = 7.3 Hz, 1H), 5.39 (dd,  $J$  = 12.1, 6.3 Hz, 1H, CH), 3.97 (dd,  $J$  = 17.4, 12.1 Hz, 1H, CH<sub>2</sub>), 3.72 – 3.65 (m, 4H, CH<sub>2</sub>), 3.18 (dd,  $J$  = 17.4, 6.3 Hz, 1H, CH<sub>2</sub>), 3.09 – 3.01 (m, 4H, CH<sub>2</sub>). MS (EI): 418.1 (M<sup>+</sup>).

#### 4.4.8

##### **4-(4-(5-(3-Chlorophenyl)-1-phenyl-4,5-dihydro-1H-pyrazol-3-yl)phenyl)morpholine (4h)**

Yellow crystal, yield 80.6%, m.p. 146-148 °C. <sup>1</sup>H NMR (400 MHz, DMSO-*d*<sub>6</sub>)  $\delta$  7.93 (d,  $J$  = 7.4 Hz, 1H, ArH), 7.72 (d,  $J$  = 7.9 Hz, 1H, ArH), 7.55 (d,  $J$  = 7.9 Hz, 1H, ArH), 7.49 – 7.34 (m, 3H, ArH), 7.15 (dd,  $J$  = 13.5, 8.1 Hz, 3H, ArH), 7.04 (d,  $J$  = 7.8 Hz, 1H, ArH), 6.91 (t,  $J$  = 9.5 Hz, 2H, ArH), 6.73 (t,  $J$  = 7.2 Hz, 1H, ArH), 5.44 (dd,  $J$  = 12.2, 6.1 Hz, 1H, CH), 3.85 (dd,  $J$  = 17.4, 12.3 Hz, 1H, CH<sub>2</sub>), 3.71 (dd,  $J$  = 11.0, 6.9 Hz, 4H, CH<sub>2</sub>), 3.18 – 3.02 (m, 5H, CH<sub>2</sub>). MS (EI): 418.1 (M<sup>+</sup>).

#### 4.4.9

##### **4-(4-(5-(4-Chlorophenyl)-1-phenyl-4,5-dihydro-1H-pyrazol-3-yl)phenyl)morpholine (4i)**

Yellow crystal, yield 47.8%, m.p. 129-130 °C. <sup>1</sup>H NMR (400 MHz, DMSO-*d*<sub>6</sub>)  $\delta$  7.74 (d,  $J$  = 8.6 Hz, 2H, ArH), 7.48 (d,  $J$  = 8.6 Hz, 2H, ArH), 7.20 (s, 2H, ArH), 7.14 (dd,  $J$  = 20.0, 12.4 Hz, 4H, ArH), 7.01 (d,  $J$  = 7.9 Hz, 2H, ArH), 6.72 (t,  $J$  = 7.2 Hz, 1H, ArH), 5.45 (dd,  $J$  = 12.0, 6.0 Hz, 1H, CH), 3.93 – 3.84 (m, 1H, CH<sub>2</sub>), 3.80 (d,  $J$  = 17.8 Hz, 4H, CH<sub>2</sub>), 3.17 (s, 4H, CH<sub>2</sub>), 3.07 (dd,  $J$  = 17.5, 6.3 Hz, 1H, CH<sub>2</sub>). MS (EI): 418.1 (M<sup>+</sup>).

#### 4.4.10

##### **4-(4-(5-(3,4-Dichlorophenyl)-1-phenyl-4,5-dihydro-1H-pyrazol-3-yl)phenyl)morpholine (4j)**

Yellow crystal, yield 50.7%, m.p. 153-154 °C. <sup>1</sup>H NMR (400 MHz, DMSO-*d*<sub>6</sub>)  $\delta$  7.91 (d,  $J$  = 1.7 Hz, 1H, ArH), 7.69 (dt,  $J$  = 18.0, 5.1 Hz, 2H, ArH), 7.14 (dd,  $J$  = 14.4, 8.4 Hz, 4H, ArH), 7.04 (d,  $J$  = 7.9 Hz, 2H, ArH), 6.89 (d,  $J$  = 8.7 Hz, 2H, ArH), 6.73 (t,  $J$  = 7.2 Hz, 1H, ArH), 5.44 (dd,  $J$  = 12.2, 6.2 Hz, 1H, CH), 3.84 (dd,  $J$  = 17.6, 12.3 Hz, 1H, CH<sub>2</sub>), 3.73 – 3.65 (m, 4H, CH<sub>2</sub>), 3.15 – 3.07 (m, 1H, CH<sub>2</sub>), 3.07 – 3.00 (m, 4H, CH<sub>2</sub>). MS (EI): 451.0 (M<sup>+</sup>).

**4.4.11****4-(4-(1-Phenyl-5-(3,4,5-trichlorophenyl)-4,5-dihydro-1H-pyrazol-3-yl)phenyl)morpholine (4k)**

Yellow crystal, yield 46.4%, m.p. 166-167 °C. <sup>1</sup>H NMR (400 MHz, DMSO-*d*<sub>6</sub>) δ 7.72 (dd, *J* = 26.5, 8.7 Hz, 2H, ArH), 7.17 (t, *J* = 8.1 Hz, 4H, ArH), 7.04 (d, *J* = 7.8 Hz, 2H, ArH), 6.90 (d, *J* = 8.7 Hz, 2H, ArH), 6.76 (t, *J* = 7.3 Hz, 1H, ArH), 5.46 (dd, *J* = 12.2, 6.3 Hz, 1H, CH), 4.01 (dd, *J* = 17.5, 12.2 Hz, 1H, CH<sub>2</sub>), 3.75 – 3.66 (m, 4H, CH<sub>2</sub>), 3.21 (dd, *J* = 17.4, 6.3 Hz, 1H, CH<sub>2</sub>), 3.11 – 3.02 (m, 4H, CH<sub>2</sub>). MS (EI): 485.0 (M<sup>+</sup>).

**4.4.12****4-(4-(5-(3-Iodophenyl)-1-phenyl-4,5-dihydro-1H-pyrazol-3-yl)phenyl)morpholine (4l)**

Yellow crystal, yield 41.1%, m.p. 167-169 °C. <sup>1</sup>H NMR (400 MHz, DMSO-*d*<sub>6</sub>) δ 7.79 (d, *J* = 8.4 Hz, 2H, ArH), 7.53 (d, *J* = 8.4 Hz, 2H, ArH), 7.15 (t, *J* = 8.5 Hz, 4H, ArH), 7.02 (d, *J* = 7.9 Hz, 2H, ArH), 6.90 (d, *J* = 8.6 Hz, 2H, ArH), 6.72 (t, *J* = 7.3 Hz, 1H, ArH), 5.41 (dd, *J* = 12.2, 6.3 Hz, 1H, CH), 3.84 (dd, *J* = 17.4, 12.3 Hz, 1H, CH<sub>2</sub>), 3.76 – 3.65 (m, 4H, CH<sub>2</sub>), 3.19 – 2.92 (m, 5H, CH<sub>2</sub>). MS (EI): 508.9 (M<sup>+</sup>).

**4.4.13****4-(4-(1-Phenyl-5-(*m*-tolyl)-4,5-dihydro-1H-pyrazol-3-yl)phenyl)morpholine (4m)**

Yellow crystal, yield 73.0%, m.p. 138-141 °C. <sup>1</sup>H NMR (400 MHz, DMSO-*d*<sub>6</sub>) δ 7.60 (s, 1H, ArH), 7.53 (d, *J* = 7.4 Hz, 1H, ArH), 7.32 (t, *J* = 7.6 Hz, 1H, ArH), 7.16 (dd, *J* = 18.2, 9.4 Hz, 5H, ArH), 7.02 (d, *J* = 7.8 Hz, 2H, ArH), 6.90 (d, *J* = 8.7 Hz, 2H, ArH), 6.71 (t, *J* = 7.2 Hz, 1H, ArH), 5.39 (dd, *J* = 12.1, 5.9 Hz, 1H, CH), 3.85 (dd, *J* = 17.2, 12.0 Hz, 1H, CH<sub>2</sub>), 3.70 (d, *J* = 4.6 Hz, 4H, CH<sub>2</sub>), 3.07 (dd, *J* = 11.2, 6.3 Hz, 5H, CH<sub>2</sub>), 2.36 (s, 3H, CH<sub>3</sub>). MS (EI): 397.1 (M<sup>+</sup>).

**4.4.14 4-(4-(1-Phenyl-5-(*p*-tolyl)-4,5-dihydro-1H-pyrazol-3-yl)phenyl)morpholine (4n)**

Yellow crystal, yield 65.9%, m.p. 134-135 °C. <sup>1</sup>H NMR (400 MHz, DMSO-*d*<sub>6</sub>) δ 7.63 (d, *J* = 8.1 Hz, 2H, ArH), 7.23 (d, *J* = 8.0 Hz, 2H, ArH), 7.13 (dt, *J* = 7.2, 3.5 Hz, 4H, ArH), 7.00 (d, *J* = 7.9 Hz, 2H, ArH), 6.88 (d, *J* = 8.7 Hz, 2H, ArH), 6.69 (t, *J* =

7.2 Hz, 1H, ArH), 5.34 (dd,  $J = 12.0, 6.3$  Hz, 1H, CH), 3.83 (dd,  $J = 17.4, 12.1$  Hz, 1H, CH<sub>2</sub>), 3.72 – 3.66 (m, 4H, CH<sub>2</sub>), 3.09 – 2.99 (m, 5H, CH<sub>2</sub>), 2.33 (s, 3H, CH<sub>3</sub>). MS (EI): 397.1 (M<sup>+</sup>).

#### 4.4.15

#### 4-(4-(1-Phenyl-5-(4-(trifluoromethyl)phenyl)-4,5-dihydro-1H-pyrazol-3-yl)phenyl)morpholine (4o)

Yellow crystal, yield 76.3%, m.p. 151-153 °C. <sup>1</sup>H NMR (400 MHz, DMSO-*d*<sub>6</sub>)  $\delta$  7.73 (d,  $J = 7.9$  Hz, 2H, ArH), 7.47 (d,  $J = 8.4$  Hz, 2H, ArH), 7.14 (dd,  $J = 13.3, 6.0$  Hz, 4H, ArH), 7.02 (d,  $J = 7.9$  Hz, 2H, ArH), 6.88 (d,  $J = 7.4$  Hz, 2H, ArH), 6.71 (t,  $J = 7.2$  Hz, 1H, ArH), 5.39 (s, 1H, CH), 3.82 (t,  $J = 14.8$  Hz, 1H, CH<sub>2</sub>), 3.69 (s, 4H, CH<sub>2</sub>), 3.04 (s, 5H, CH<sub>2</sub>). MS (EI): 451.2 (M<sup>+</sup>).

#### 4.4.16

#### 4-(4-(5-(2-Methoxyphenyl)-1-phenyl-4,5-dihydro-1H-pyrazol-3-yl)phenyl)morpholine (4p)

Yellow crystal, yield 68.4%, m.p. 183-185 °C. <sup>1</sup>H NMR (400 MHz, DMSO-*d*<sub>6</sub>)  $\delta$  7.89 (d,  $J = 7.7$  Hz, 1H, ArH), 7.36 (t,  $J = 7.1$  Hz, 1H, ArH), 7.14 (t,  $J = 7.7$  Hz, 4H, ArH), 7.08 (d,  $J = 8.3$  Hz, 1H, ArH), 7.01 (dd,  $J = 11.4, 8.0$  Hz, 3H, ArH), 6.90 (d,  $J = 8.5$  Hz, 2H, ArH), 6.70 (t,  $J = 7.2$  Hz, 1H, ArH), 5.30 (dd,  $J = 11.9, 6.4$  Hz, 1H, CH), 3.91 (dd,  $J = 10.3, 7.5$  Hz, 1H, CH<sub>2</sub>), 3.80 (s, 3H, CH<sub>3</sub>), 3.73 – 3.67 (m, 4H, CH<sub>2</sub>), 3.20 – 3.02 (m, 5H, CH<sub>2</sub>). MS (EI): 413.1 (M<sup>+</sup>).

#### 4.4.17

#### 4-(4-(5-(3-Methoxyphenyl)-1-phenyl-4,5-dihydro-1H-pyrazol-3-yl)phenyl)morpholine (4q)

Yellow crystal, yield 56.5%, m.p. 179-180 °C. <sup>1</sup>H NMR (400 MHz, DMSO-*d*<sub>6</sub>)  $\delta$  7.91 (s, 1H), 7.71 (d,  $J = 7.9$  Hz, 1H, ArH), 7.54 (d,  $J = 7.9$  Hz, 1H, ArH), 7.40 (ddd,  $J = 11.6, 10.0, 5.0$  Hz, 3H, ArH), 7.16 – 7.11 (m, 3H, ArH), 7.03 (d,  $J = 7.8$  Hz, 1H, ArH), 6.90 (t,  $J = 9.5$  Hz, 2H, ArH), 6.72 (t,  $J = 7.2$  Hz, 1H, ArH), 5.43 (dd,  $J = 12.2, 6.1$  Hz, 1H, CH), 3.90 (dd,  $J = 10.3, 7.5$  Hz, 1H, CH<sub>2</sub>), 3.78 (s, 3H, CH<sub>3</sub>), 3.72 – 3.66 (m, 4H, CH<sub>2</sub>), 3.18 – 3.01 (m, 5H, CH<sub>2</sub>). MS (EI): 413.1 (M<sup>+</sup>).

#### 4.4.18

**4-(4-(5-(4-Methoxyphenyl)-1-phenyl-4,5-dihydro-1H-pyrazol-3-yl)phenyl)morpholine (4r)**

Yellow crystal, yield 56.5%, m.p. 177-179 °C. <sup>1</sup>H NMR (400 MHz, DMSO-*d*<sub>6</sub>) δ 7.57 (d, *J* = 8.9 Hz, 2H, ArH), 7.37 – 7.29 (m, 3H, ArH), 7.09 (dd, *J* = 8.7, 3.1 Hz, 4H, ArH), 7.03 (s, 2H, ArH), 6.98 (dd, *J* = 8.0, 3.8 Hz, 1H, ArH), 6.89 (s, 1H, ArH), 5.54 (dd, *J* = 12.0, 4.9 Hz, 1H, CH), 3.89 (dd, *J* = 17.6, 12.0 Hz, 1H, CH<sub>2</sub>), 3.81 (s, 3H, CH<sub>3</sub>), 3.71 – 3.65 (m, 4H, CH<sub>2</sub>), 3.15 (dd, *J* = 17.6, 5.0 Hz, 1H, CH<sub>2</sub>), 3.07 – 3.01 (m, 4H, CH<sub>2</sub>). MS (EI): 413.1 (M<sup>+</sup>).

**4.4.19****4-(4-(5-(2-Nitrophenyl)-1-phenyl-4,5-dihydro-1H-pyrazol-3-yl)phenyl)morpholine (4s)**

Red crystal, yield 39.2%, m.p. 179-181 °C. <sup>1</sup>H NMR (400 MHz, DMSO-*d*<sub>6</sub>) δ 8.09 (s, 1H, ArH), 7.72 (d, *J* = 7.9 Hz, 2H, ArH), 7.23 (t, *J* = 7.8 Hz, 1H, ArH), 7.19 – 7.11 (m, 4H, ArH), 7.03 (d, *J* = 7.9 Hz, 2H, ArH), 6.89 (d, *J* = 8.7 Hz, 2H, ArH), 6.73 (t, *J* = 7.3 Hz, 1H, ArH), 5.42 (dd, *J* = 12.2, 6.1 Hz, 1H, CH), 3.84 (dd, *J* = 17.5, 12.3 Hz, 1H, CH<sub>2</sub>), 3.73 – 3.68 (m, 4H, CH<sub>2</sub>), 3.12 – 3.03 (m, 5H, CH<sub>2</sub>). MS (EI): 428.1 (M<sup>+</sup>).

**4.4.20****4-(4-(5-(3-Nitrophenyl)-1-phenyl-4,5-dihydro-1H-pyrazol-3-yl)phenyl)morpholine (4t)**

Red crystal, yield 48.9%, m.p. 176-178 °C. <sup>1</sup>H NMR (400 MHz, DMSO-*d*<sub>6</sub>) δ 8.26 (d, *J* = 9.0 Hz, 2H, ArH), 7.96 (d, *J* = 8.9 Hz, 2H, ArH), 7.18 (ddd, *J* = 37.2, 19.1, 8.2 Hz, 8H, ArH), 6.79 (t, *J* = 7.2 Hz, 1H, ArH), 5.61 (dd, *J* = 12.5, 6.1 Hz, 1H, CH), 3.94 (dd, *J* = 17.5, 12.5 Hz, 1H, CH<sub>2</sub>), 3.80 (s, 4H, CH<sub>2</sub>), 3.16 (dd, *J* = 17.6, 5.8 Hz, 5H, CH<sub>2</sub>). MS (EI): 428.1 (M<sup>+</sup>).

**4.5 Antibacterial activity<sup>26</sup>**

Two Gram-negative bacterial strains: *E. coli* ATCC 25922 and *P. aeruginosa* ATCC 27853 and two Gram-positive bacterial strains: *B. subtilis* ATCC 530 and *S. aureus* ATCC 25923 were employed in the antibacterial activities test, using method recommended by National Committee for Clinical Laboratory Standards (NCCLS).

By two-fold serial dilution method, the *in vitro* activities of the compounds were tested in Nutrient broth (NB) for bacteria. Seeded broth (broth containing microbial spores) was prepared in NB from 24 h-old bacterial cultures on nutrient agar (Hi-media) at 37 °C. The bacterial suspension was adjusted with sterile saline to a concentration of  $1 \times 10^4$ – $10^5$  CFU/mL. The tested compounds and reference drugs were prepared by two-fold serial dilution to obtain the required concentrations of 100, 50, 25, 12.5, 6.25, 3.13, 1.56, 0.78  $\mu\text{g/mL}$ . The tubes were incubated in BOD incubators at 37 °C for bacteria. The MICs were recorded by visual observations after 24 h (for bacteria) of incubation. Kanamycin B and penicillin were used as standards for bacterial. The observed MICs are presented in **Table 1**.

#### 4.6 Preparation of the TyrRS and enzyme assay

*S. aureus* TyrRS enzyme was over-expressed in *E. coli* bacteria and purified to near homogeneity (~98% as judged by SDS–PAGE) using standard purification procedures. TyrRS activity was measured by aminoacylation using modifications to previously described methods. The assays were performed at 37 °C in a mixture containing (final concentrations) 100 mM Tris/Cl pH 7.9, 50 mM KCl, 16 mM  $\text{MgCl}_2$ , 5 mM ATP, 3 mM DTT, 4 mg/ml *E. coli* MRE600 tRNA (Roche) and 10  $\mu\text{M}$  L-tyrosine (0.3  $\mu\text{M}$  L-[ring-3,5- $^3\text{H}$ ] tyrosine (PerkinElmer, Specific activity: 1.48 - 2.22 TBq/mmol), 10  $\mu\text{M}$  carrier). TyrRS (0.2 nM) was pre-incubated with a range of inhibitor concentrations for 10 min at room temperature followed by the addition of pre-warmed mixture at 37 °C. After specific intervals, the reaction was terminated by adding aliquots of the reaction mix into ice-cold 7% trichloroacetic acid and harvesting onto 0.45 mm hydrophilic Durapore filters (Millipore Multiscreen 96-well plates) and counted by liquid scintillation. The rate of reaction in the experiments was linear with respect to protein and time with less than 50% total tRNA acylation.  $\text{IC}_{50}$  values correspond to the concentration at which half of the enzyme activity is inhibited by the compound. The results are presented in **Table 2**.

#### 4.7 Cytotoxicity test

Cells were incubated in a 96-well plate at a density of  $10^5$  cells per well with various concentrations of compounds for 48 h. For the cytotoxicity assay, 20  $\mu\text{L}$  of MTT (5 mg/mL) was added per well 4 h before the end of the incubation. After removing the supernatant, 200  $\mu\text{L}$  DMSO was added to dissolve the formazan crystals. The absorbance at  $\lambda 570$  nm was read on an ELISA reader (Tecan, Austria).

#### 4.8 Experimental protocol of docking study

Molecular docking of compound **4s** into the three dimensional X-ray structure of *S. aureus* TyrRS (PDB code: 1JIJ) was carried out using the Discovery Studio (version 3.5) as implemented through the graphical user interface DS-CDOCKER protocol. The three-dimensional structures of the aforementioned compounds were constructed using Chem. 3D ultra 12.0 software [Chemical Structure Drawing Standard; Cambridge Soft corporation, USA (2010)], then they were energetically minimized by using MMFF94 with 5000 iterations and minimum RMS gradient of 0.10. The crystal structures of protein complex were retrieved from the RCSB Protein Data Bank (<http://www.rcsb.org/pdb/home/home.do>). All bound waters and ligands were eliminated from the protein. The molecular docking was performed by inserting compound **4s** into the binding pocket of *S. aureus* TyrRS based on the binding mode. Types of interactions of the docked protein with ligand-based pharmacophore model were analyzed after the end of molecular docking.

#### 4.9 3D-QSAR

Ligand-based 3D-QSAR approach was performed by QSAR software of DS 3.5 (Discovery Studio 3.5, Accelrys, Co.Ltd). The training sets were composed of inhibitors with the corresponding  $\text{pIC}_{50}$  values which were converted from the obtained  $\text{IC}_{50}$  ( $\mu\text{M}$ ), and test sets comprised compounds of data sets as list in **Table 4**. All the definition of the descriptors can be seen in the “Help” of DS 3.5 software and they were calculated by QSAR protocol of DS 3.5. The alignment conformation of each molecule was the one with lowest interaction energy in the docked results of CDOCKER. The predictive ability of 3D-QSAR modeling can be evaluated based on

the cross-validated correlation coefficient, which qualifies the predictive ability of the models. Scrambled test (Y scrambling) was performed to investigate the risk of chance correlations. The inhibitory potencies of compounds were randomly reordered for 30 times and subject to leave-one-out validation test, respectively. The models were also validated by test sets, in which the compounds are not included in the training sets.

### Acknowledgment

The work was financed by a grant (No. J1103512) from National Natural Science Foundation of China.

### References

1. Z. P. Xiao, X. D. Wang, P. F. Wang, Y. Zhou, J. W. Zhang, L. Zhang, J. Zhou, S. S. Zhou, H. Ouyang, X. Y. Lin, M. Mustapa, A. Reyinbaike and H. L. Zhu, *European journal of medicinal chemistry*, 2014, **80**, 92-100.
2. T. Nasr, S. Bondock and S. Eid, *European journal of medicinal chemistry*, 2014, **84**, 491-504.
3. G. H. Vondenhoff and A. Van Aerschot, *European journal of medicinal chemistry*, 2011, **46**, 5227-5236.
4. M. K. Kathiravan, A. B. Salake, A. S. Chothe, P. B. Dudhe, R. P. Watode, M. S. Mukta and S. Gadhwé, *Bioorganic & medicinal chemistry*, 2012, **20**, 5678-5698.
5. M. F. El-Behairy, T. E. Mazeed, A. A. El-Azzouny and M. N. Aboul-Enein, *Saudi Pharmaceutical Journal*, 2014, DOI: 10.1016/j.jsps.2014.07.009.
6. D. J. Payne, M. N. Gwynn, D. J. Holmes and D. L. Pompliano, *Nature reviews. Drug discovery*, 2007, **6**, 29-40.
7. C. R. Woese, G. J. Olsen, M. Ibba and D. Soll, *Microbiology and molecular biology reviews : MMBR*, 2000, **64**, 202-236.
8. S. F. Wang, Y. Yin, F. Qiao, X. Wu, S. Sha, L. Zhang and H. L. Zhu, *Bioorganic & medicinal chemistry*, 2014, **22**, 2409-2415.

9. A. Zask, J. Kaplan, J. C. Verheijen, D. J. Richard, K. Curran, N. Brooijmans, E. M. Bennett, L. Toral-Barza, I. Hollander, S. Ayril-Kaloustian and K. Yu, *Journal of medicinal chemistry*, 2009, **52**, 7942-7945.
10. P. Panneerselvam, R. R. Nair, G. Vijayalakshmi, E. H. Subramanian and S. K. Sridhar, *European journal of medicinal chemistry*, 2005, **40**, 225-229.
11. D. V. Dekhane, S. S. Pawar, S. Gupta, M. S. Shingare, C. R. Patil and S. N. Thore, *Bioorg Med Chem Lett*, 2011, **21**, 6527-6532.
12. A. Smelcerovic, M. Rangelov, Z. Smelcerovic, A. Veljkovic, E. Cherneva, D. Yancheva, G. M. Nikolic, Z. Petronijevic and G. Kocic, *Food and chemical toxicology : an international journal published for the British Industrial Biological Research Association*, 2013, **55**, 493-497.
13. A. McGhee, B. M. Cochran, T. A. Stenmark and F. E. Michael, *Chemical communications*, 2013, **49**, 6800-6802.
14. A. P. Keche, G. D. Hatnapure, R. H. Tale, A. H. Rodge and V. M. Kamble, *Bioorg Med Chem Lett*, 2012, **22**, 6611-6615.
15. Z. Ozdemir, H. B. Kandilci, B. Gumusel, U. Calis and A. A. Bilgin, *European journal of medicinal chemistry*, 2007, **42**, 373-379.
16. J. G. Lombardino and I. G. Otterness, *Journal of medicinal chemistry*, 1981, **24**, 830-834.
17. M. Shaharyar, A. A. Siddiqui, M. A. Ali, D. Sriram and P. Yogeewari, *Bioorg Med Chem Lett*, 2006, **16**, 3947-3949.
18. T. Chandra, N. Garg, S. Lata, K. K. Saxena and A. Kumar, *European journal of medicinal chemistry*, 2010, **45**, 1772-1776.
19. J. H. Ahn, H. M. Kim, S. H. Jung, S. K. Kang, K. R. Kim, S. D. Rhee, S. D. Yang, H. G. Cheon and S. S. Kim, *Bioorg Med Chem Lett*, 2004, **14**, 4461-4465.
20. A. H. Banday, B. P. Mir, I. H. Lone, K. Suri and H. Kumar, *Steroids*, 2010, **75**, 805-809.
21. G. Wanare, R. Aher, N. Kawathekar, R. Ranjan, N. K. Kaushik and D. Sahal, *Bioorg Med Chem Lett*, 2010, **20**, 4675-4678.
22. X. Wang, Y. M. Pan, X. C. Huang, Z. Y. Mao and H. S. Wang, *Organic & biomolecular chemistry*, 2014, **12**, 2028-2032.
23. J. J. Liu, J. Sun, Y. B. Fang, Y. A. Yang, R. H. Jiao and H. L. Zhu, *Organic & biomolecular*

- chemistry*, 2014, **12**, 998-1008.
24. Z. P. Xiao, H. Ouyang, X. D. Wang, P. C. Lv, Z. J. Huang, S. R. Yu, T. F. Yi, Y. L. Yang and H. L. Zhu, *Bioorganic & medicinal chemistry*, 2011, **19**, 3884-3891.
25. H.-Y. Qiu, Z.-C. Wang, P.-F. Wang, X.-Q. Yan, X.-M. Wang, Y.-H. Yang and H.-L. Zhu, *RSC Advances*, 2014, **4**, 39214.
26. J.-J. Liu, J. Sun, Y.-B. Fang, Y.-A. Yang, R.-H. Jiao and H.-L. Zhu, *Organic & biomolecular chemistry*, 2014, **12**, 998-1008.

### Figure Captions

**Table 1.** Antibacterial activities (MIC,  $\mu\text{g/mL}$ ) of target compounds (**4a-4t**)

**Table 2.** *S. aureus* TyrRS enzyme inhibition ( $\text{IC}_{50}$ ,  $\mu\text{M}$ ) and cytotoxicity ( $\text{CC}_{50}$ ,  $\mu\text{M}$ ) data of all compounds

**Table 3.** Experimental, predicted inhibitory activity of compounds **4a-4t** by 3D-QSAR models based upon active conformation achieved by molecular docking

**Figure 1.** Morpholine-containing drugs

**Figure 2.** 2D docking model of interactions between compound **4s** with *S. aureus* TyrRS enzyme.

**Figure 3.** 3D docking model of interactions between compound **4s** with *S. aureus* TyrRS enzyme: for clarity, only interacting residues are displayed.

**Figure 4.** Plot of experimental vs. predicted *S. aureus* TyrRS enzyme inhibitory activities of training set and test set.

**Figure 5.** (a) 3D QSAR model coefficients on electrostatic potential grids. Blue represents positive coefficients; red represents negative coefficients. (b) 3D QSAR model coefficients on van der Waals grids. Green represents positive coefficients; yellow represents negative coefficients.

**Scheme 1.** General synthesis of compounds (**4a-4t**). Reagents and conditions: (a) 1.0 equiv *p*-fluorobenzaldehyde, DMSO, reflux 4 h; (b) 1.0 equiv acetophenones, 3.0 equiv KOH,  $\text{CH}_3\text{CH}_2\text{OH}$ ,  $0^\circ\text{C}$ , 2 h; (c) 1.22 equiv phenylhydrazine, acetic acid, reflux, 6 h.

**Table 1.** Antibacterial activities (MIC  $\mu\text{g/mL}$ ) of target compounds (**4a-4t**)

Compounds	R	MIC( $\mu\text{g/mL}$ )			
		Gram-positive		Gram-negative	
		<i>B. subtilis</i>	<i>S. aureus</i>	<i>P. aeruginosa</i>	<i>E. coli</i>
<b>4a</b>		12.50	12.50	12.50	25.00
<b>4b</b>		3.13	3.13	3.13	6.25
<b>4c</b>		6.25	3.13	6.25	12.50
<b>4d</b>		12.50	6.25	12.50	25.00
<b>4e</b>		3.13	3.13	3.13	6.25
<b>4f</b>		3.13	6.25	3.13	6.25
<b>4g</b>		6.25	12.50	12.50	12.50
<b>4h</b>		6.25	3.15	6.25	12.50
<b>4i</b>		12.50	6.25	12.50	12.50
<b>4j</b>		6.25	6.25	12.50	12.50
<b>4k</b>		6.25	6.25	12.50	6.25
<b>4l</b>		12.50	12.50	12.50	12.50
<b>4m</b>		12.50	6.25	12.50	25.00
<b>4n</b>		12.50	12.50	12.50	12.50
<b>4o</b>		6.25	6.25	3.13	6.25
<b>4p</b>		12.50	12.50	6.25	12.50
<b>4q</b>		12.50	6.25	12.50	12.50
<b>4r</b>		12.50	12.50	12.50	12.50

<b>4s</b>		1.56	0.78	3.13	1.56
<b>4t</b>		1.56	3.13	3.13	6.25
<b>Penicillin</b>	-	3.13	3.13	1.56	3.13
<b>Kanamycin</b>	-	1.56	1.56	3.13	1.56

**Table 2.** *S. aureus* TyrRS enzyme inhibition ( $IC_{50}$ ,  $\mu M$ ) and cytotoxicity ( $CC_{50}$ ,  $\mu M$ ) data of all compounds

Compounds	$CC_{50}^a$ ( $\mu M$ )		$IC_{50}^a$ ( $\mu M$ )
	Cytotoxic		<i>S. aureus</i> TyrRS $IC_{50}$
<b>4a</b>	291.05		48.79
<b>4b</b>	204.71		11.92
<b>4c</b>	200.00		4.53
<b>4d</b>	182.48		15.27
<b>4e</b>	202.41		18.28
<b>4f</b>	231.07		22.52
<b>4g</b>	227.40		30.73
<b>4h</b>	225.22		24.10
<b>4i</b>	195.35		32.22
<b>4j</b>	207.90		30.99
<b>4k</b>	197.88		5.75
<b>4l</b>	176.24		42.08
<b>4m</b>	259.31		39.09
<b>4n</b>	223.62		18.13
<b>4o</b>	194.06		12.34
<b>4p</b>	230.10		21.67

<b>4q</b>	242.93	17.16
<b>4r</b>	220.07	20.38
<b>4s</b>	221.36	1.63
<b>4t</b>	252.19	3.72

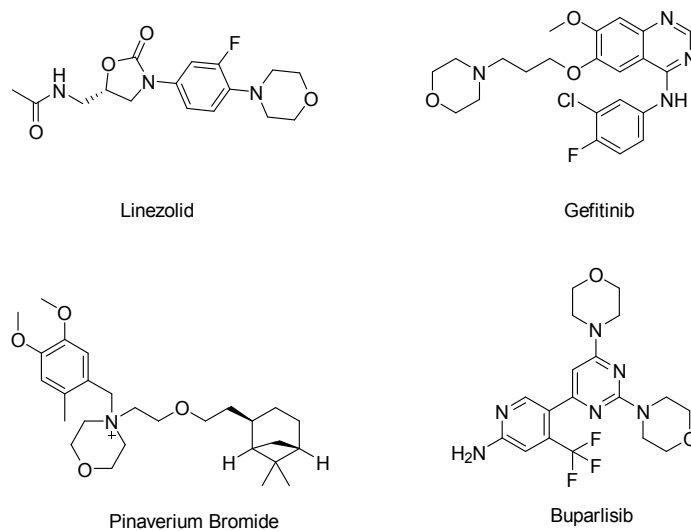
<sup>a</sup> Values are the average of three independent experiments run in triplicate. Variation was generally 5-10%.

**Table 3.** Experimental, predicted inhibitory activity of compounds **4a-t** by 3D-QSAR models based upon active conformation achieved by molecular docking.

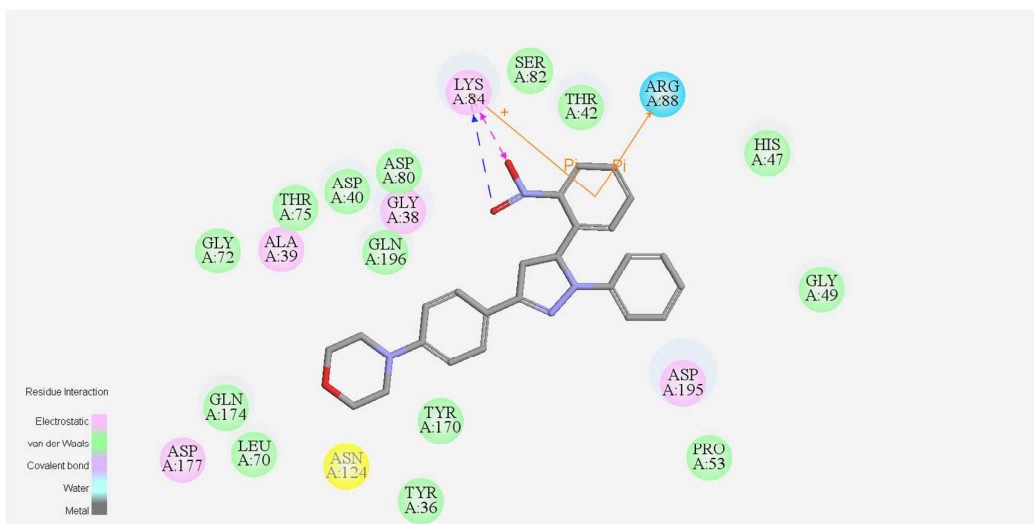
Compound <sup>a</sup>	Actual pIC <sub>50</sub>	Predicted pIC <sub>50</sub>	Residual error
<b>4a</b>	4.31	4.34	-0.03
<b>4b</b>	4.92	4.89	-0.03
<b>4c</b>	5.34	5.32	0.02
<b>4d</b>	4.82	4.77	0.04
<b>4e</b>	4.74	4.95	-0.22
<b>4f</b>	4.65	4.66	-0.01
<b>4g</b>	4.51	4.74	-0.23
<b>4h</b>	4.62	4.56	0.06
<b>4i</b>	4.49	4.67	-0.18
<b>4j</b>	4.51	5.15	-0.64
<b>4k</b>	5.24	5.34	-0.10
<b>4l</b>	4.38	4.38	0.00
<b>4m</b>	4.41	4.78	-0.37
<b>4n</b>	4.74	4.47	0.26
<b>4o</b>	4.91	4.81	0.09
<b>4p</b>	4.66	4.71	-0.05

<b>4q</b>	4.77	4.79	-0.03
<b>4r</b>	4.69	4.50	0.19
<b>4s</b>	5.79	5.55	0.24
<b><u>4t</u></b>	5.43	5.13	0.29

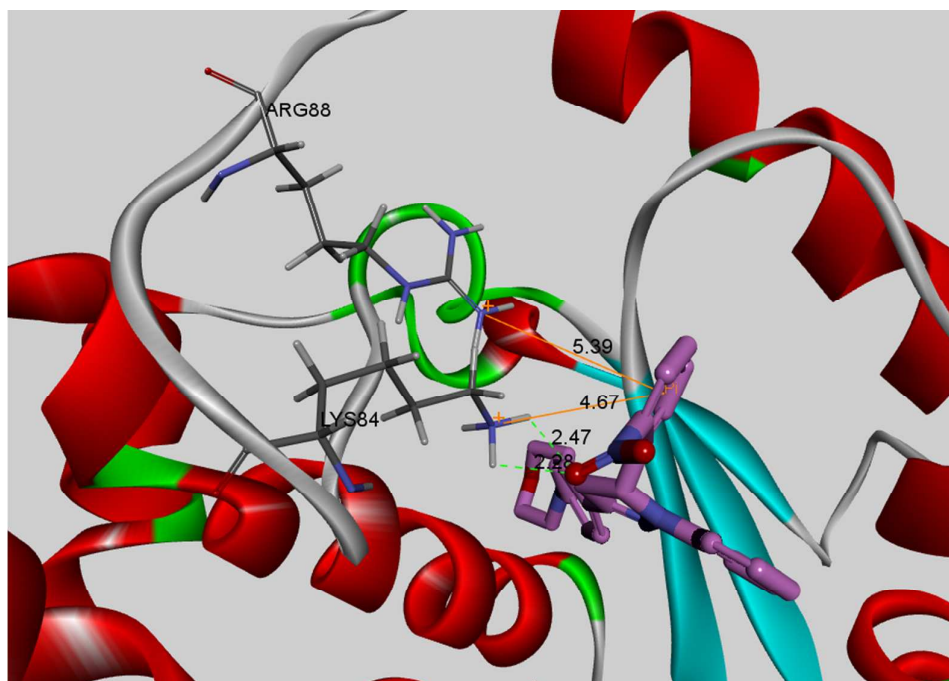
<sup>a</sup> The underlined for the test set, and the rest for training.



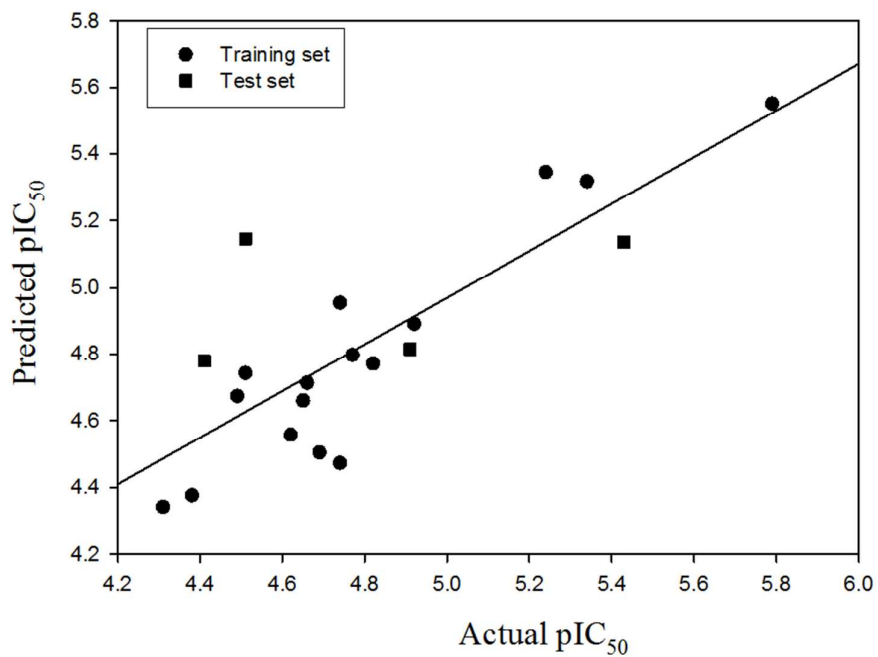
**Figure 1.** Morpholine-containing drugs



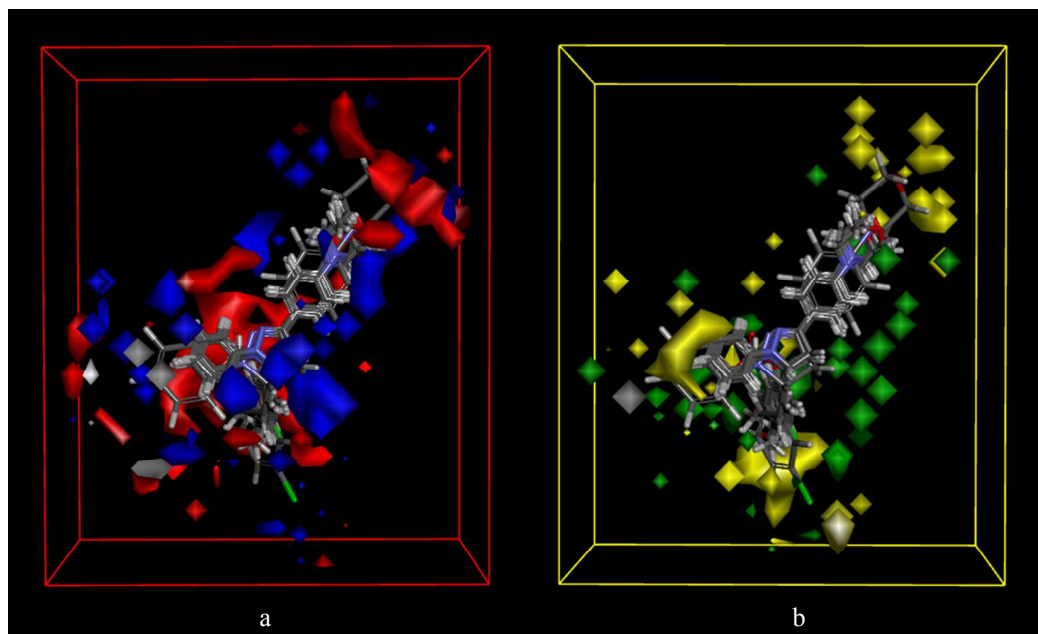
**Figure 2.** 2D docking model of interactions between compound **4s** with *S. aureus* TyrRS enzyme.



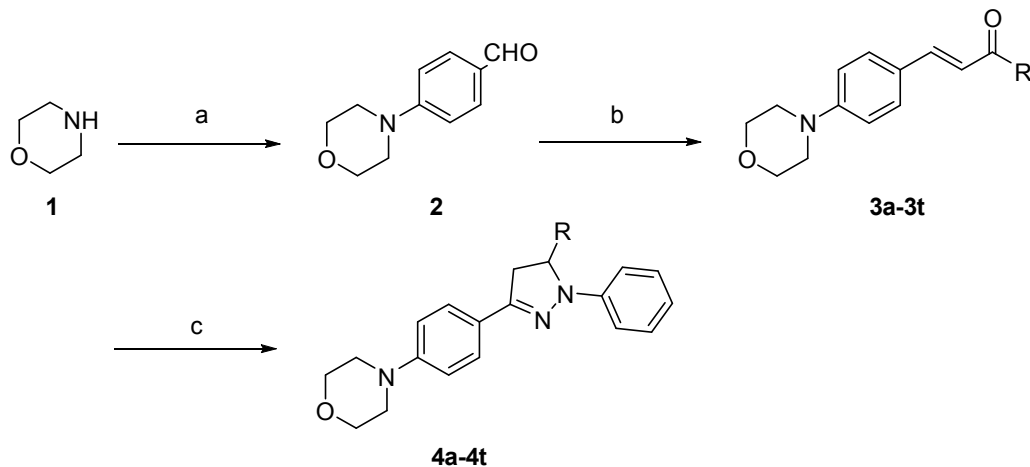
**Figure 3.** 3D docking model of interactions between compound 4s with *S. aureus* TyrRS enzyme: for clarity, only interacting residues are displayed.



**Figure 4.** Plot of experimental vs. predicted *S. aureus* TyrRS enzyme inhibitory activities of training set and test set.



**Figure 5.** (a) 3D QSAR model coefficients on electrostatic potential grids. Blue represents positive coefficients; red represents negative coefficients. (b) 3D QSAR model coefficients on van der Waals grids. Green represents positive coefficients; yellow represents negative coefficients.



**Scheme 1.** General synthesis of compounds (**4a-4t**). Reagents and conditions: (a) 1.0 equiv *p*-fluorobenzaldehyde, DMSO, reflux 4 h; (b) 1.0 equiv acetophenones, 3.0 equiv KOH, CH<sub>3</sub>CH<sub>2</sub>OH, 0°C, 2 h; (c) 1.22 equiv phenylhydrazine, acetic acid, reflux, 6 h.